The Future of Gas Turbine Technology
8th International Gas Turbine Conference
12-13 October 2016, Brussels, Belgium

Paper ID Number (57-IGTC16)

EXPERIMENTAL INVESTIGATION RESULTS OF A HYBRID CERAMIC AND ACTIVELY COOLED BALL BEARING FOR GAS TURBINES

Peter Glöckner*, Matthias Martin*, Michael Flouros**

*FAG Aerospace GmbH & Co.KG
Georg-Schäfer-Str. 30, 97421 Schweinfurt, Germany
peter.gloeckner@schaeffler.com, matthias.martin@schaeffler.com

**MTU Aero Engines AG
Dachauer Str. 665, 80995 Munich, Germany
michael.flouros@mtu.de

ABSTRACT

Rolling element bearings are one of the components which significantly determine the reliability and mechanical efficiency of aerospace engines and drive trains as well as stationary gas turbines. They have to withstand very demanding operating conditions. Especially main shaft ball bearings in modern aircraft engines and stationary gas turbines experience high rotational speeds, loads and temperatures. In addition, rolling element bearings installed in aircraft engines have to meet the highest reliability requirements.

Increasing bearing rotational speeds and thrust load density contribute to a higher thermal efficiency of today's and future gas turbines. This development trend translates into increased bearing power losses and temperatures, which demand increased cooling oil quantities. These are connected with higher power losses due to oil churning. Thus, the requirements for future gas turbine ball bearings are reduced power losses, bearing and oil temperatures as well as increased reliability. Here, maintenance free components for stationary gas turbines and "power by the hour" requirements for aircraft engines play an important role.

In this article, the experimental investigation results for a novel gas turbine ball bearing are presented. The investigated bearing features ceramic balls, direct outer ring cooling, squeeze film damping and surface nitrided raceways. These material and design attributes contribute to increased efficiency, robustness and reliability. Rig testing under typical aircraft engine flight conditions has been performed in order to investigate the influence on bearing power loss, temperatures and cooling efficiency. The fundamental experimental results including oil and bearing temperature distribution, power dissipation and bearing efficiency as well as the technology transfer into stationary gas turbines are presented.

Keywords
Rolling Element Bearings, Gas Turbines, Aircraft Engines, Cooling, Ceramics, Mechanical Efficiency

INTRODUCTION

Next generation gas turbines for aircraft and oil and gas applications will run at higher speeds and thrust load density. Increased rotor speeds lead to higher contact friction power in the bearing rolling contacts and therefore increase the bearing temperatures. This, on the one hand, leads to reduced endurance strength of the bearing materials (Böhmer et al., 1999). On the other hand, higher temperatures reduce the oil film thickness between the rolling contact surfaces and increase the probability of asperity contacts (Gloeckner et al., 2009). Gloeckner and Ebert (2010) have shown that the phenomenon of micro-sliding significantly contributes to surface initiated fatigue for high speed all-steel ball bearings. For hybrid ball bearings, i.e. bearings featuring steel raceways and ceramic balls, the influence of this phenomenon on heat generation and surface fatigue is not known as of today.

In order to cool the bearing below the critical temperatures, higher oil quantities are required. Higher oil quantities again increase the oil churning losses. The amount of churning losses represent typically 60-80 % of the total power loss for gas turbine main shaft ball bearings. In addition, higher oil quantities demand larger periphery oil system components, such as pumps, oil feed and scavenge lines, heat exchanger, etc.

Therefore the goal for next generation gas turbine ball bearings is the reduction of power losses and bearing

temperature at significant higher rotor speeds. This can be achieved by new design concepts, materials, and heat treatment technologies.

One approach to reduce the rolling contact friction power is to utilize ceramic balls made out of silicon nitride (Si_3N_4) material. Ebert (1990) and Forster et al. (2011) already reported temperature and power loss reductions for high speed hybrid ball bearings. However, the mechanism is not fully understood and requires further research. Furthermore ceramic balls offer a 56 % weight benefit over steel balls, especially valuable to aero engines and helicopter applications. The weight advantage is alleviated as the Young's modulus of silicon nitride is 60 % higher compared with steel. This translates in smaller contact zones and increased Hertzian stress for the same geometry and external loads. Higher Hertzian stresses and contact friction power can be tolerated with higher strength material. Therefore the investigated ball bearing features duplex-hardened raceways. This means the raceways experience a surface-near nitriding process at the end of the manufacturing process. The duplex-hardened raceways develop high surface-near compressive residual stress and high hardness resulting in reduced equivalent stresses and higher material strength. Duplex-hardened bearings are proven to show superior performance over conventional M50 and M50NiL bearing material, in particular in the mixed friction regime and under hard-particle contamination (Streit et al., 2006).

The reduction of oil churning power losses can be achieved by decreased oil quantities supplied into the bearing. Only a minor portion of the oil supplied is required for lubrication, the vast majority is used for cooling. Therefore separating cooling and lubrication fluids would be the optimal method to achieve this. The direct outer ring cooling concept represents a technology to (partially) decouple lubrication and cooling oil. Gloeckner et al. (2011) experimentally investigated the direct outer ring cooling concept for an all-steel bearing. A cooling channel in the bearing outer ring outer diameter enables temperature reductions of 20 K, oil mass flow reductions up to 50 % and bearing power loss reduction up to 25 %.

As aircraft gas turbine experience additional vibrational loads, today's aero engines feature integrated squeeze film dampers between bearing and housing. Thus, critical engine structures are protected by viscous damping. The investigated ball bearing features an integrated squeeze film damper between outer ring outer diameter and housing inner diameter.

The combination of the direct outer ring cooling concept, ceramic balls and the integrated squeeze film damper represents a high potential to enable very high bearing speeds at low temperatures and power losses.

Rig testing of the novel ball bearing was performed on the FAG aircraft engine bearing test rig in close cooperation with MTU. During rig testing, shaft speeds of 24000 rpm corresponding to speed indices over $4 \cdot 10^6$ mm/min were achieved. The speed index is the product of bearing pitch diameter (U.S. bore diameter) and rotational speed. State of the art gas turbine ball bearings achieve speed indices up to $3.2 \cdot 10^6$ mm/min.

This is the first time, a gas turbine main shaft ball bearing operates at equal or higher speed indices. This accomplishment represents a major milestone in the development of next generation high speed ball bearings and was acknowledged by international news agencies (Toensmeier, 2015). The experimental investigation results are presented in the next chapters.

NOMENCALTURE

c_p	Mean specific heat capacity
F_{Thrust}	Bearing axial load
h	heat transfer coefficient
HTO	Heat to oil
$m_{W,left}$	Oil mass flow to the left bearing side
$m_{W,right}$	Oil mass flow to the right bearing side
m_{nom}	Nominal oil mass flow supplied by under-race lubrication
n	Rotational speed
P_{Total}	Total bearing power loss
p_0	Max. Hertzian stress
$T_{i,OilOut,left}$	Under-race oil out temperature to the left bearing side
$T_{i,OilOut,right}$	Under-race oil out temperature to the right bearing side
$T_{o,Bulk,loaded}$	Outer ring bulk temperature on the right (loaded) bearing side
$T_{o,Bulk,unloaded}$	Outer ring bulk temperature on the left (unloaded) bearing side
$T_{i,Bulk,loaded}$	Bulk temperature on the left (loaded) inner ring half
$T_{i,Bulk,unloaded}$	Bulk temperature on the right (unloaded) inner ring half
$T_{o,Oil,left}$	Oil temperature on the left bearing side
$T_{o,Oil,right}$	Oil temperature on the right bearing side
T_{OilIn}	Oil inlet temperature
$T_{o,OilOut}$	Outer ring channel oil out temperature (bypass scavenge temperature)
V_{nom}	Nominal oil volume flow supplied by under-race lubrication
V_o	Outer ring channel oil volume flow (bypass oil flow)
ξ	Oil out flow ratio on the left bearing side
η	Scoop efficiency
ρ	Oil density

TEST RIG AND TEST BEARING CONFIGURATION

Fig. 1 displays the investigated ball bearing. Compared with the all-steel bearing used to investigate the direct outer ring cooling concept (Gloeckner, 2011), the squeeze film damper, ceramic balls and the duplex-hardened raceways differ. The internal geometry is identical to the all-steel bearing.

Fig. 1: Cutaway of the investigated ball bearing

The helical cooling channel (Fig 2, top right) in the outer diameter of the inward outer ring features the same cross section and length as for the all-steel bearing. The novel ball bearing features an additional outer ring (Fig. 2, top left) around the bearing allowing for squeeze film damping between housing inner diameter and bearing outer diameter. The oil for the outer ring cooling channel is provided via oil holes in the side face of the outward outer ring. This ring also features piston ring grooves. The piston rings on the forward and aft side seal the squeeze oil film between outer ring and housing. Fig. 2 also depicts a cut-up of inward and outward outer ring with the helical cooling channel and the squeeze film damper grooves visible.

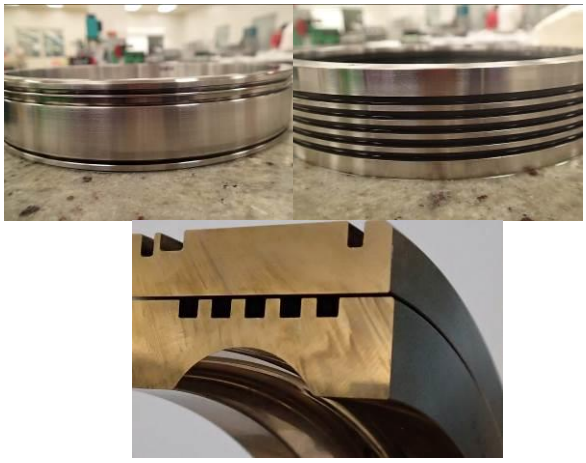

Fig. 2: outward outer ring (top left) with piston ring and oil distribution grooves, inward outer ring with cooling channel (top right), cut-up of the combined outer ring (bottom)

For the bearing raceways M50NiL material as per AMS6278 was used. The cage is made out of AMS6414 steel, bearing a sliver plating in accordance with AMS2412. The cage/ball assembly in Fig. 3 shows the 22.225 mm (7/8") size ceramic balls after the test run. The under-race lubrication is ensured by 6 radial oil grooves in the split face of the loaded inner ring half (Fig. 3, top left). Furthermore, the outer ring and the whole bearing assembly after rig-testing are shown in Fig. 3. After rig testing a visual and dimensional inspection of all bearing components was performed. No indications or anomalies were detected.

Fig. 3: Rig tested components of the investigated hybrid ball bearing: inner ring half (top left), cage/ball assembly (top right), outer ring (bottom left) and bearing assembly (bottom right)

A cross section of the test bearing and the bearing chamber with the measured variables is shown in Figure 4.

The squeeze film damper oil is provided by a radial oil supply line through the bearing housing, not shown in the cross section of Fig. 4. The oil flow in the outer ring channel V_o is also provided by a radial oil supply line. Oil-in and oil-out of the helical cooling channel are 30° offset. The oil flow direction in the helical channel is from the bearing's right side (Opposite Drive End) to the bearing's left side (Drive End). This facilitates direct heat transfer from the loaded outer ring side to the cooling oil in the channel. The oil feed to the outer ring cooling channel is sealed on both sides in order to impede radial oil leakages.

Thermocouples were applied to the inner and outer ring bulk material, both on the loaded and unloaded sides. The position of the thermocouples in the outer and inner ring is identical to the thermocouple position in the all-steel bearing investigated by Gloeckner et al. (2011). The bearing bulk temperatures were measured at three circumferential positions each. In Fig. 3, the holes in the inward outer ring for the thermocouples can be viewed.

The thermocouples installed axially close to the cage side faces on the left and the right bearing side ($T_{o,Oil,left}$ and $T_{o,Oil,right}$) provide the actual oil temperatures used to calculate the heat to oil (HTO) for the inner oil circuit and indicate the heat distribution in the axial direction. With the temperatures measured by thermocouples before and after the cooling channel (T_{OilIn} and $T_{o,OilOut}$) the HTO for the outer oil circuit (bypass) is calculated. In order to

investigate the effect of the squeeze film damper leakage oil flow on the oil scavenge temperature, thermocouples at the bearing chamber oil exits were installed ($T_{i,Oilout,left}$ and $T_{i,Oilout,right}$). In addition, the oil mass flow was measured on the left and right side of the bearing in order to monitor bearing pumping action, a phenomenon comprehensively investigated and described by Flouros (2004). The influence of the squeeze film damping on bearing chamber vibration was controlled by axial, radial and tangential acceleration sensors on both the drive end and the opposite drive end side of the bearing chamber. For completion, the bearing chamber oil out temperatures were measured. The total bearing power loss was recorded by a high speed torque meter during all operating conditions.

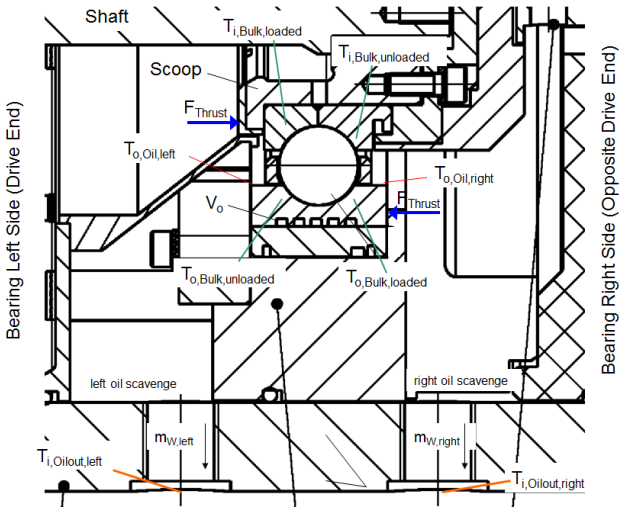

Fig. 4: Rig tested hybrid ball bearing and bearing chamber with measured variables

The hybrid ball bearing was axially loaded in a thrust range of 26.7 kN to 80 kN. As indicated in Fig. 4, the left inner ring half and the outer ring's right side were loaded. Rotational speeds were varied between 8000 and 24000 rpm. For the investigated load and speed range the Hertzian stress varied between 1650 to 2540 MPa on the inner raceway and 1520 to 2260 MPa on the outer raceway. The rotational speed of 24000 rpm is equivalent to a speed index of $D_m \cdot n = 4.02 \cdot 10^6$ mm/min (U.S. $3.2 \cdot 10^6$ mm/min). The speed range investigated is in the upper range and beyond state of the art aircraft engine rolling bearings, exceeding for the first time a speed index of $4 \cdot 10^6$ mm/min. The nominal bearing under-race oil flow was varied between 5 and 15 l/min and the cooling oil flow through the outer ring channel was varied between 0 and 3 l/min. The oil in temperature is identical for the outer ring cooling channel, the squeeze film damper and the under-race lubrication. The oil used in this investigation meets the requirements of MIL-PRF 23699.

Figure 5 shows the maximum theoretical Hertzian stress on the inner and outer ring raceways for both the hybrid and the all-steel bearing. For the hybrid bearing, the measured bulk temperatures (see Fig. 4) were considered to calculate the internal radial clearance (operating contact angles). For the steel bearing, the bulk temperatures obtained by Gloeckner et al. (2011) were extrapolated. At lower rotational speeds, the inner and outer ring raceways of the all-steel bearing are equally loaded. In contrast, the Hertzian stress differs by approximately 150 MPa between inner and outer ring raceway for the hybrid bearing. Due to the higher density of the steel ball, the centrifugal forces lead to significant high stresses on the outer ring raceway of the all-steel bearing at very high rotational speeds. At the same time the stress difference between inner and outer ring raceway is larger than 150 MPa, while the raceways of the hybrid bearing are equally low loaded. This emphasizes the expected advantages of hybrid bearings at high speeds and moderate loads.

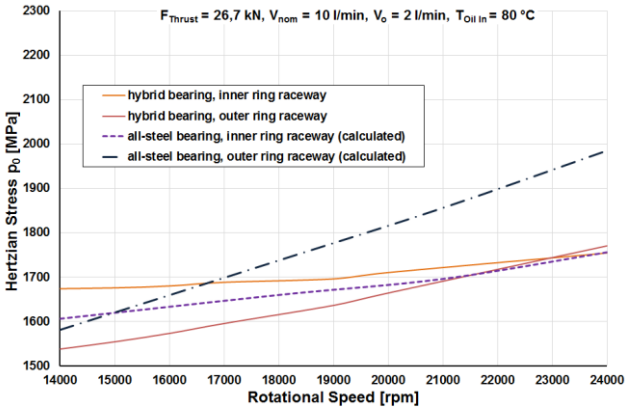

Fig. 5: Hertzian stresses for the hybrid and the all-steel bearing

In the following chapter the rig testing results for the investigated hybrid ball bearing are presented and compared with the experimental results for the all-steel bearing. More than 300 load cases were investigated. Therefore, a broad range of operating conditions was covered, simulating real aircraft engine operating conditions.

TESTING RESULTS

In this section, the experimental results including bulk and oil temperatures, oil flow distribution, heat to oil and bearing power loss are presented as functions of the various operating conditions. The influence of the new design and material is presented. The results are compared directly with the data presented by Gloeckner et al. (2011) and Flouros et al. (2012).

Oil Feed Efficiency and Oil Distribution

The oil feed efficiency or scoop efficiency (equation (1)) is an important factor which describes how much nominal provided oil is actually transported into the bearing.

$$\eta = \frac{m_{W,left} + m_{W,right}}{m_{nom}} \quad (1)$$

The effective amount of oil directly influences the bearing bulk temperatures, oil out temperatures and therefore the transferred heat to oil (HTO). In order to compare the all-steel with the hybrid ball bearing, the amount of oil effectively supplied by under-race into the bearing should be identical for both configurations. As the amount of effective oil supplied into the bearing varies depending on speed and oil scoop geometry for under-race lubricated bearings and neither the scoop geometry nor the bearing under-race lubrication features were changed compared to the all-steel bearing, the scoop efficiency shows similar values for the hybrid bearing, Fig 6.

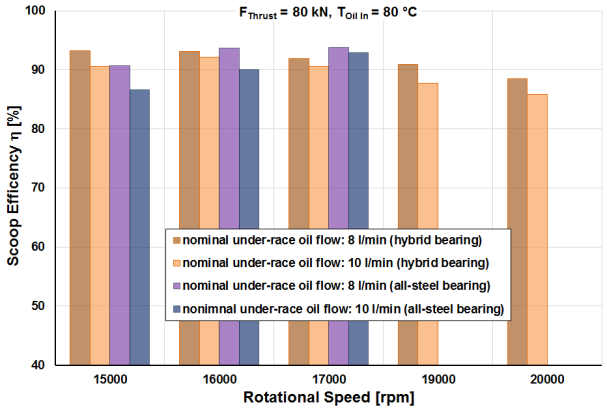

Fig. 6: Scoop Efficiency for the hybrid and all-steel bearings

For both configurations the scoop efficiency is higher for lower under-race oil quantities. The larger the nominal oil flow quantity, the more windage losses occur at the injection point below the scoop. This effect is characteristic for high speed under-race lubrication. However, based on the very similar scoop efficiency results, the direct comparison of both bearing configurations is feasible.

In Fig. 7, the ratio of the oil out flow on the left side of the bearing and to the total bearing oil out flow is shown. The ratio is calculated per equation (2).

$$\xi = \frac{m_{W,left}}{m_{W,left} + m_{W,right}} \quad (2)$$

For the hybrid and all-steel bearing, between 73 and 80 % of the effective supplied oil is transported ("pumped") to the left side of the bearing, i.e. into the direction of the axial load flow. Already Flouros (2004) and Gloeckner et al. (2011) found that the major portion of the nominal supplied under-race oil is "pumped" into the axial load direction and also contains the higher temperature. As no significant differences between hybrid and steel bearing occur, the ring bulk and oil temperatures of both bearing versions can be directly compared. These are presented in the following chapter

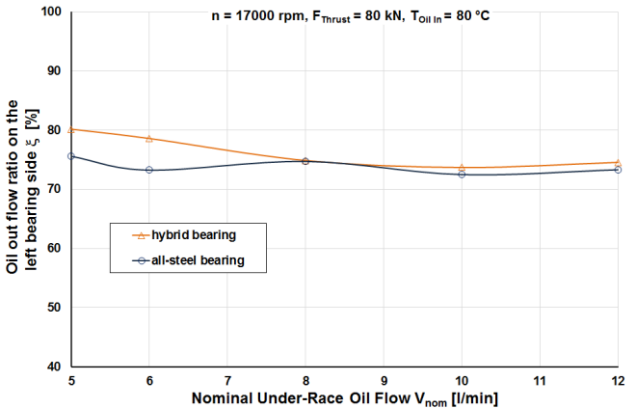

Fig. 7: Oil out flow ratio (bearing left side)

Temperatures

Conventionally, the bearing ring temperature is controlled by the nominal under-race oil flow quantity. It is the most significant variable to achieve oil churning loss reductions. Fig. 8 shows that the mean outer ring temperature can be reduced by more than 25 K for the all-steel bearing and by more than 30 K for the hybrid bearing if the under-race oil flow is increased from 5 to 12 l/min. Simultaneously the power losses are increased. This relation is discussed in the following chapter (cf. Fig. 15).

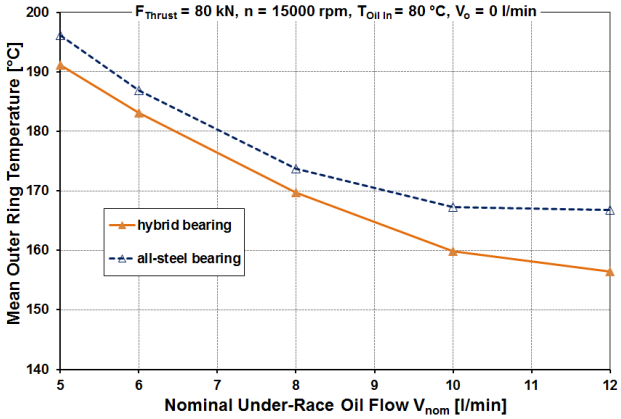

Fig. 8: Influence of under-race oil flow on mean bearing outer ring temperature

It is clearly visible in Fig. 8 that the hybrid bearing offers additional temperature benefits for larger oil flows. Corresponding to the preliminary considerations (Fig. 5), the outer ring bulk temperature of the hybrid bearing is reduced between 5 and 8 K (Fig. 9). This can be explained by the lower centrifugal forces acting on the outer ring raceway contacts. This effect may be weakened for very high loads, when the Hertzian stress is dominated by the external loads.

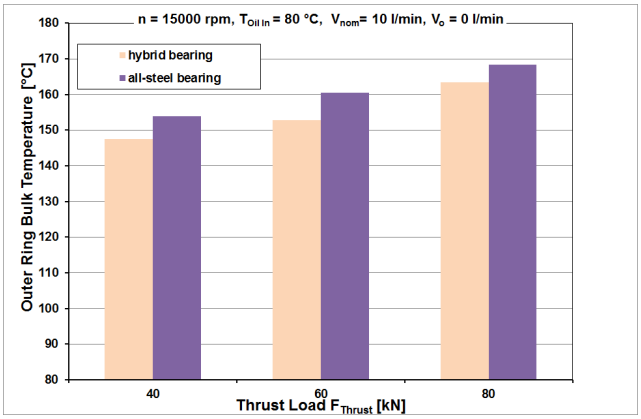

Fig. 9: Influence of bearing thrust load on outer ring bulk temperature

Lower outer ring temperatures increase the rolling contact endurance strength threshold. Moreover, they contribute to higher oil viscosity and oil density (Mihailidis, 2002) and can increase the oil film thickness within the rolling contact. Thus, the rolling contact material stressing and the friction power dissipated within the rolling contacts can be reduced.

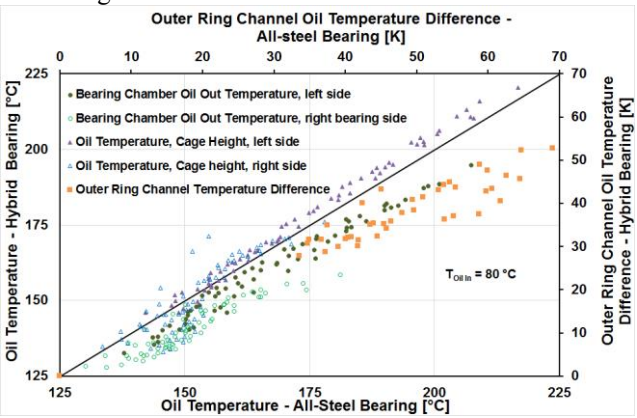

Fig. 10: Comparison of hybrid and all-steel bearing oil temperatures

Besides the bearing ring temperatures, the oil temperatures are an important indicator for the heat load distribution and are required to calculate the power, which is transferred into the cooling oil. In Fig. 10 the oil temperatures close to the cage ($T_{o,Oil,left}$, $T_{o,Oil,right}$), the bearing chamber oil out temperatures ($T_{i,Oilout,left}$, $T_{i,Oilout,right}$) and the temperature difference between outer ring channel oil inlet and oil outlet are shown ($T_{o,Oilout}$ - T_{OilIn}). The oil temperature close to the bearing cage on the left side is on average higher for the hybrid bearing, while it is on average lower on the right bearing side. The hybrid bearing ”pumps” slightly higher oil quantities to the left bearing side (cf. Fig. 7). The bearing chamber oil out temperatures show for all load cases lower temperatures for the hybrid bearing. The squeeze film damper piston rings allow for a small oil leakage flow to the left and right bearing side. Therefore the bearing chamber oil out temperature is reduced when bearing oil out flow and squeeze film damper oil leakage flow mix. This does not necessarily mean that the total heat to oil is higher for the hybrid bearing configuration since the leakage mass flows need to be considered in the energy balance (see next section).

Furthermore it can be seen from Fig. 10, that the temperature difference between the outer ring cooling channel oil inlet and oil outlet temperature is lower for the hybrid bearing. This means less heat is transferred from the outer ring material into the channel, considering that the channel geometry is identical compared with the all-steel bearing. This is a consequence of the lower centrifugal forces and reduced Hertzian stresses for the hybrid bearing. In Fig. 11 the outer ring channel oil out temperature is shown for various rotational speeds depending on the outer ring channel oil flow. The temperature gradients for the hybrid bearing are lower, in particular for low outer ring channel oil flows of 1 l/min. The gradient increases for higher rotational speeds of 19000 and 20000 rpm, because more heat is generated in the outer ring raceway rolling contacts. This means the outer ring cooling channel is more efficient at high rotational speeds for the hybrid bearing.

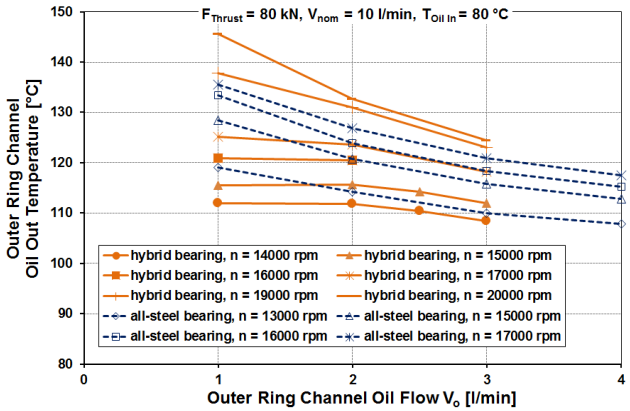

Fig. 11: Outer ring channel scavenge temperature

The influence of the outer ring channel cooling oil flow on the bearing bulk temperatures is presented in Fig. 12. For an outer ring channel oil flow of 1 l/min, the maximum outer ring temperature is reduced by 6.3 K. increasing the oil flow to 3 l/min results in a total temperature reduction of 13.2 K. The inner ring temperature on the loaded side also benefits from the cooler outer ring. The inner ring temperature is reduced by approximately 1.5 K/l. Thus, the cooling channel is efficient. Compared with the all-steel bearing, the temperature reductions are smaller due to the lower heat load from the outer ring raceway.

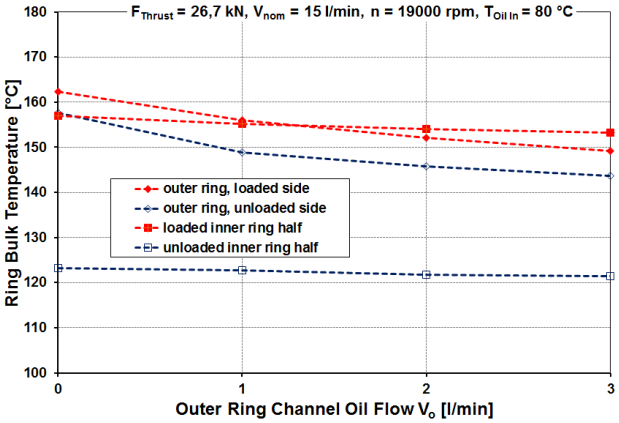

Fig. 12: Influence of outer ring channel oil flow on outer ring and inner ring bulk temperatures of the investigated hybrid bearing

The experimentally obtained ring and oil temperatures point to a high efficiency of the hybrid bearing outer ring cooling channel for very high speeds. In the following section the transferred heat to oil and the total bearing power loss are discussed in order to gain a wider understanding of the hybrid bearing efficiency.

Energy Dissipation

The temperature difference between oil in and oil out for the under-race lubrication and the outer ring cooling channel determines the heat to oil for the inner (HTO_i) and outer oil circuit (HTO_o). The combined heat to oil of both circuits describes the dissipated power, which can be directly compared with the all-steel bearing.

The HTO_i consists of the heat to oil transferred into the oil out flow on the left bearing side ($HTO_{i,l}$), on the right bearing side ($HTO_{i,r}$) and into the rejected oil ($HTO_{i,ro}$), which is not transported into the bearing inward (eq. (3)).

$$HTO_i = HTO_{i,l} + HTO_{i,r} + HTO_{i,ro} \tag{3}$$

The heat to oil transferred into the outer ring cooling channel (HTO_o) is important to determine the amount of heat transferred from the dissipated power in the outer ring raceway contacts into the channel cooling oil. Together with the inner circuit heat to oil it yields the total heat to oil:

$$HTO = HTO_i + HTO_o \tag{4}$$

For the calculation of each heat to oil in eq. (3) and (4), the respective oil temperatures and oil mass flows as per Fig. 4 need to be used. The specific heat capacity c_p is used for the mean oil temperature.

$$HTO = m_w \cdot c_p \cdot (T_{Oilout} - T_{OilIn}) \tag{5}$$

As applicable to the all-steel bearing, the required pumping power for the under-race lubrication and the outer ring cooling channel can be neglected for the investigated oil flow range.

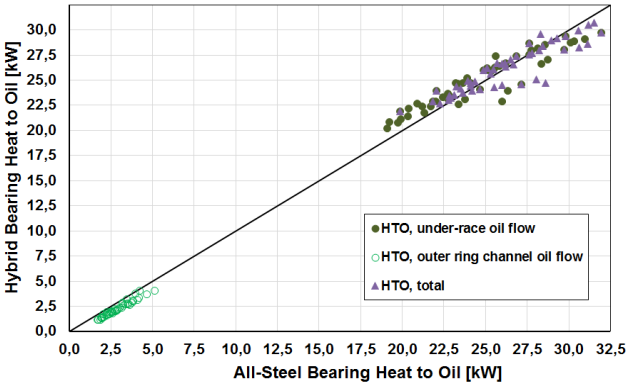

Fig. 13: Comparison of hybrid and all-steel bearing heat to oil (HTO)

Fig. 13 compares the heat to oil for the hybrid bearing with the all-steel bearing. Both the individual oil circuits and the combination per eq. (4) are considered. The same results as shown in Fig. 11 apply for the hybrid bearing cooling channel: The lower amount of heat is transferred into the channel due to the lower friction energy dissipated in the outer ring raceway contacts. For the majority of the investigated load cases, slightly more total heat is transferred into the oil for the hybrid bearing. The inner ring raceways experience higher Hertzian stresses (cf. Fig. 4) due to the higher Young's modulus of the ceramic balls. Therefore the lower contact friction power in the outer ring ring contacts is neutralized by higher friction power in the inner ring raceway contacts. In the design stage, this effect must be considered by enhanced inner ring cooling designs, such as axial oil grooves, oil scallops in the bore diameter or radial oil holes to the inner ring shoulders.

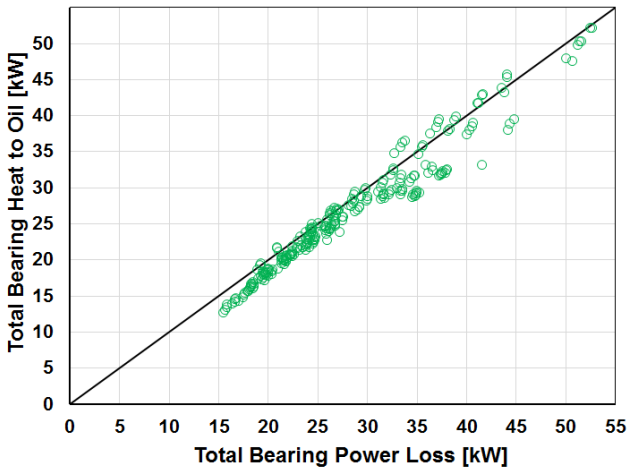

Fig. 14: Comparison of calculated heat to oil and measured power loss for the investigated hybrid ball bearing

The validity of the calculated HTO can be verified by comparison with the measured power loss. In this investigation a high speed torque meter was used to measure the total bearing friction for all load cases. Fig. 14 shows a good match of the calculated heat to oil and the measured power loss. The measured power loss is underestimated by 6 % on average for all load cases. This means that heat radiation from the bearing and heat conduction into the surrounding components are negligible. Therefore HTO can be used to evaluate the oil mass and power loss savings which can be achieved for the hybrid bearing with the outer ring cooling channel.

As already discussed, the under-race oil flow quantity is the key parameter to achieve reductions of bearing power loss and to partially decouple lubrication and cooling. Fig. 15 clearly shows the influence of high under-race oil flows on the total bearing power loss. This is in particular true for high rotation speeds, because oil churning increases with both rotational speed and oil quantity. For 20000 rpm and 15 l/min, the total bearing power loss was measured to 51.4 kW. Such high values represent major challenges for the entire oil system, including heat exchanger, scavenge lines, pumps, etc.

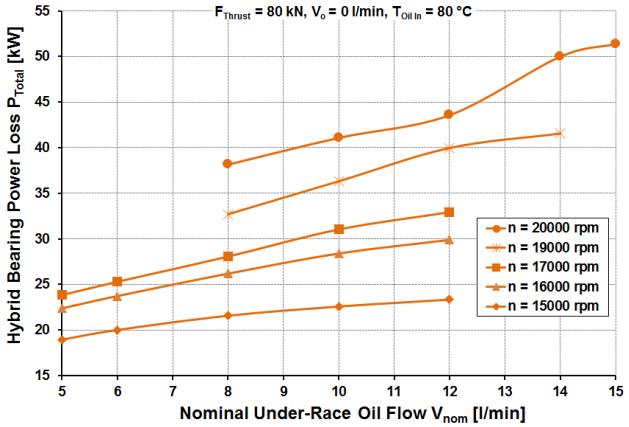

Fig. 15: Total bearing power loss (torque meter results)

Therefore it is required for future gas turbine ball bearings to operate with lower under-race oil quantities. Fig. 16 shows an approach to achieve lower bearing power losses by applying the outer ring cooling concept: For the subject load case and conventional under-race lubrication of 15 l/min the mean outer ring temperature is 160 °C. The identical temperature is adjusted by applying 2.5 l/min oil flow in the outer ring cooling channel. In return, the nominal under-race oil flow can be reduced to 8 l/min. This significant reduction of under-race oil flow of 46 % results in a total heat to oil reduction of 5.1 kW, i.e. 17 %.

The outer ring cooling concept enables significant under-race oil flow and total friction reductions. Beyond that, the high speed potential offered by the squeeze film damper and the low weight ceramic balls had to be investigated. The results for the high speed investigations are presented in the following section.

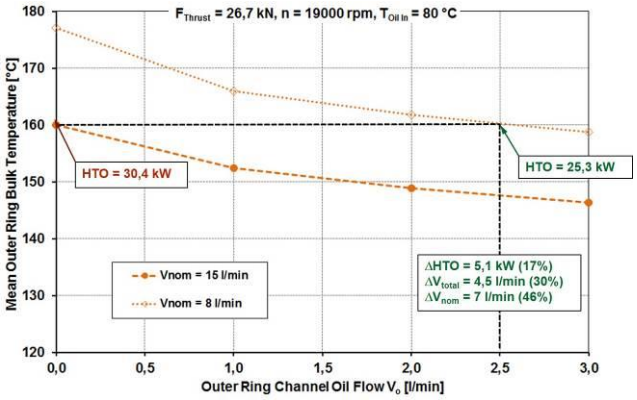

Fig. 16: Savings in oil mass flow and heat to oil by using the direct outer ring cooling concept for the hybrid bearing

High Speed Record

It was presented in the previous chapters that the hybrid ball bearing operates efficiently at high operational speeds and moderate loads. In combination with the squeeze film damper, which reduces additional vibrational loads, and the direct outer ring cooling, the hybrid bearing is suited to operate at very high speeds without significant temperature increase. In Fig. 17 the outer ring temperature, the total bearing power loss and the radial acceleration measured at the opposite drive end (ODE) side of the test head are shown. With the hybrid ball bearing rotational speeds of 24000 rpm ($D_m \cdot n = 4.02 \cdot 10^6$ mm/min) were achieved. This represents a new speed record for aircraft engine ball bearings.

Due to the outer ring cooling channel oil flow of 2 l/min and the reduced centrifugal forces, the mean outer ring temperature is only 183 °C − despite the high sum velocities acting on the rolling contacts. The power loss at 24000 rpm is 44.2 kW. It can be extrapolated from Fig. 15 that a conventionally cooled bearing lubricated with 15 l/min would require at least 10 kW higher drive power.

Moreover, the squeeze film damper helped to overcome critical eigen frequencies of the test rig at approximately 17500 rpm. The all-steel bearing without any additional squeeze film damping showed at these speeds unacceptable high vibrations. Therefore the maximum achievable rotational speed with the all-steel bearing was limited to 17000 rpm (Gloeckner et al. 2011).

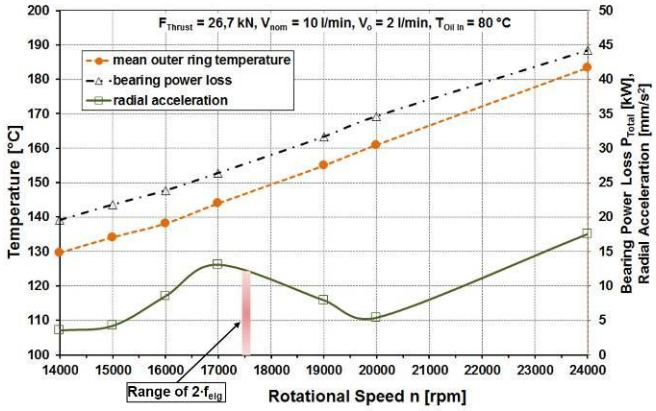

Fig. 17: Hybrid bearing temperatures and power loss for high rotational speeds

CONCLUSIONS

The identical test rig set up enabled a direct comparison of the investigated hybrid ball bearing with the previously investigated all-steel bearing.

The outer ring temperatures are slightly lower for the hybrid bearing. This measurement result correlates with lower outer ring channel oil out temperatures and lower outer ring channel heat to oil. The lower heat to oil is a consequence of less power dissipated in the outer ring raceway contacts due to lower centrifugal loading. The bulk temperatures are efficiently reduced by the outer ring cooling channel. The direct outer ring cooling efficiency increases with high speeds above 17000 rpm. I.e., the temperature gradient for the bypass oil out flow increases significantly with very high speeds.

For the majority of the investigated load cases the hybrid bearing features higher total heat to oil compared to the all-steel design. This is a results of higher inner race contact stresses occurring at high thrust loads. However, total heat to oil reductions of more than 17 % were achieved by applying the direct outer ring cooling concept. These reductions originate in significant reduced under-race oil flow quantities of more than 45 %.

For the first time, a rolling element bearing dedicated to gas turbines exceeded the speed index of 4 $\cdot 10^6$ mm/min. This was achieved by a combination of 2 l/min bypass oil flow, the low weight ceramic balls and the squeeze film damping. In summary, similar cooling efficiencies for a higher speed range and low to moderate thrust loads are achieved compared with the previous investigated all-steel bearing.

The suitability for very high speeds using only small low oil quantities qualifies the investigated hybrid bearing for the transfer into stationary gas turbine. The application on the high pressure spool and the continuous operation at high speeds allows for high power loss savings and potential smaller and cost effective oil system architecture. Furthermore the investigated bearing can be potentially transferred into similar high speed bearing applications such as machine tool or turbocharger bearings.

ACKNOWLEDGEMENTS

The authors would like to express their acknowledgment to the German Federal Ministry for Economic Affairs and Energy for the financial support within the cooperative project “Eff_ÖLS - Effective Oil Systems” FKZ 20T1101B, Research Program “Luftfahrtforschungsprogramm IV, 2012 - 2015 (LuFo)”.

REFERENCES

Böhmer, H., Lösche, T., Ebert, F. J., and Streit, E., 1999: “The Influence of Heat Generation in the Contact Zone on Bearing Fatigue Behavior,” ASME J. Tribology, 121, pp. 462–467.

Ebert, F.-J., 1990: Performance of Silicon Nitride (Si3N4) Components in Aerospace Bearing Applications. ASME, Proceedings of the Gas Turbine and Aeroengine Congress and Exposition, June 11–14, Brussels, 90-GT-166.

Flouros, M, 2004, “Oil Pumping in High Speed and High Loaded Ball Bearings”, Proceedings of ASME Turbo Expo, Vienna, Austria, GT2004-53406

Flouros M., Hirschmann, M., Cottier, F., Gloeckner P., and Dullenkopf K., 2012, “Active Outer Ring Cooling of High Loaded and High Speed Ball Bearings,” Proceedings of ASME Turbo Expo 2012, GT2012-68138.

Forster, N., Svendsen, V., Given, G., Thompson, K., Dao N., and Nicholson, B., 2011, “Parametric Testing and Heat Generation Modeling of 133-mm Bore Ball Bearings: Part II—Results with Silicon Nitride Rolling Elements,” Trib. Trans., 54, pp. 325–331.

Gloeckner, P., Sebald, W., and Bakolas V., 2009, “An Approach to Understanding Micro-Spalling in High-Speed Ball Bearings Using a Thermal Elastohydrodynamic Model”, Trib. Trans., 52, pp. 534-543.

Gloeckner, P. and Ebert, F.-J., 2010, “Micro-Sliding in High-Speed Aircraft Engine Ball Bearings,” Trib. Trans., 53, pp. 369–375.

Gloeckner P., Dullenkopf K., and Flouros M., 2011, “Direct Outer Ring Cooling of a High Speed Jet Engine Mainshaft Ball Bearing - Experimental Investigation Results,” Journal of Engineering for Gas Turbines and Power, 133/6, pp. 1-7.

Mihailidis, A., Panagiotidis, K., and Drivakos, N. 2002, “Influence of Lubricant Thermal Properties on Elastohydrodynamic Lubrication,” Proceedings of the 4th International Conference on Tribology “Balkantrib 2002”, Kayseri, Turkey, S. 41–48

Streit, E., Brock, J., and Poulin, P., 2006, “Performance Evaluation of ‘Duplex Hardened’ Bearings for Advanced Turbine Engine Applications,” Journal of ASTM International, Vol. 3, Nr. 4, West Conshohocken.

Toensmeier, P., 2015, “Cool Runnings – Turbofan bearing offers speed, fuel economy and improved engine performance,” Aviation Week and Space Technology - Defense Technology Edition, October 12-25, p. DTI4.